Heterochiral Interactions in Molecular and Macromolecular Pairs of Liquid Crystals of (*R*)- and (*S*)-2-Fluoro-4-methylpentyl 4′-((8-(Vinyloxy)octyl)oxy)biphenyl-4-carboxylate Enantiomers

Virgil Percec* and Hiroji Oda

Department of Macromolecular Science, Case Western Reserve University, Cleveland, Ohio 44106

Received January 4, 1994; Revised Manuscript Received June 15, 1994•

ABSTRACT: The synthesis and characterization of (*R*)-2-fluoro-4-methylpentyl 4′-((8-(vinyloxy)octyl)oxy)-biphenyl-4-carboxylate ((*R*)-8 (*R* >95%) and (*S*)-2-fluoro-4-methylpentyl 4′-((8-(vinyloxy)octyl)oxy)biphenyl-4-carboxylate ((*S*)-8) (*S* >95%) enantiomers and of their corresponding homopolymers and copolymers with well-defined molecular weights and narrow molecular weight distributions are presented. The phase behaviors of (*R*)-8 and poly[(*R*)-8] are identical to those of (*S*)-8 and poly[(*S*)-8], respectively. Both monomers display enantiotropic S_A and S_C* phases, a monotropic S_X (unidentified smectic) phase, and a crystalline phase, while the corresponding polymers exhibit only enantiotropic S_C* and S_X mesophases. Phase diagrams were investigated in detail for binary mixtures of (*R*)-8 with (*S*)-8 and poly[(*R*)-8] with poly[(*S*)-8] and for binary copolymers of (*R*)-8 with (*S*)-8 as a function of the composition of the two enantiomeric structural units. In all these systems the two enantiomeric structural units derived from the two monomers are miscible within all their mesophases and over the entire range of composition. The S_A–I and the K–S_C* transition temperatures of the binary mixture of (*R*)-8 with (*S*)-8 are 0.4 and 3.8 deg higher, respectively, in the 50/50 mixture than the theoretical value expected for an ideal solution, demonstrating the presence of heterochiral molecular recognition between the two enantiomers in their S_A and crystalline phases. *Heterochiral recognition in the S_C* phase, which was not detected in the monomer mixtures, was observed in the polymer mixtures.* The polymer mixtures with the lowest degree of polymerization (DP = 5) showed the largest positive deviation (*ca.* 0.5 deg) of the S_C*–I transition temperature from the ideal value. With increasing molecular weight of the polymers from the mixture, the positive deviation decreased and the chiral recognition was almost canceled at DP = 15. *In the copolymer system, chiral recognition was observed in both the S_C* and S_X phases.* The positive deviation of the S_C*–I transition temperature from the ideal value was 1.0 deg, and this value was much larger than that of the polymer mixtures with the same molecular weight (0.1–0.2 deg). *Chiral recognition in the S_X phase of copolymers is unexpected since this effect was not present in the polymer mixtures. Thus, for the first time an enhancement of chiral molecular recognition was observed in copolymers.*

Introduction

Molecular recognition is a process involving both noncovalent *binding* and *selection* of a substrate by a given receptor molecule, as well as possibly a specific function.[1] The mechanisms via which various intermolecular interactions and selection processes are generated and involved in molecular recognition were reviewed.[1a–d]

Enantiomers are considered to be perfect physical and chemical models for each other since their properties, with the exception of the rotation of polarized light and those that involve their interactions with other chiral systems, are identical. Therefore, specific noncovalent interactions between two enantiomers can be easily detected when they form an ideal solid or liquid solution as a positive deviation from the ideal behavior of any physical parameter used for their characterization. The interpretation of the phase diagrams of mixtures of enantiomers and diastereomers is discussed in detail elsewhere.[2]

Chiral molecular recognition is concerned with the investigation of the specific interactions between stereocenters.[3] The most notable series of studies on chiral molecular recognition was performed on two-dimensional monolayers of mixtures of enantiomers and diastereomers.[3b,c] The investigation of chiral interactions in crystalline materials is more difficult since melting and crystallization are kinetically controlled phase transitions. Liquid crystalline phase transitions are thermodynamically controlled, and therefore, liquid crystals facilitate the investigation of chiral recognition processes. In addition, chiral interactions in liquid crystals are of technological interest since they determine some of the most important physical properties of chiral phases such as S_C, S_A, and N.[4]

There are only a few investigations on the influence of enantiomeric excess on various phase transitions of low molar mass liquid crystals. Positive deviations from ideal values were observed for the S_A–isotropic (I) (ΔT = +0.3 deg,[5a] ΔT = +2.8 deg,[5b] ΔT = +1.0 deg,[5c] ΔT = +3.2 deg and 5.6 deg,[5d]), N–I (ΔT = +2.5 deg),[5b] S_C*–S_A (ΔT = +0.3 deg,[5b] ΔT = +0.8 and 0.5 deg)[5d] phase transitions. There is only one example in which relatively large deviations from the ideal values were observed (i.e., ΔT = +13 deg for N–I and ΔT = +5 deg for S–I phase transitions).[5e] Other mixtures of enantiomeric liquid crystals show nonideal[5f,g] or ideal[5h,i] behavior. Although the influence of enantiomeric interactions on the transition temperature of liquid crystalline phases are very low,[5] their corresponding effect on the physical parameters of chiral mesophases such as the spontaneous polarization of a S_C* phase is very large.[4b]

Presently, there is no good understanding of how the absence or the presence of enantiomeric interactions and their extent influence the physical properties of chiral liquid crystals.[4b] At the same time there are no investigations which elaborate how the structure of a stereocenter affects its interactions.

Recently, we initiated a research program to investigate chiral molecular recognition in both molecular and macromolecular pairs of enantiomeric and diastereomeric liquid crystals. The purpose of this research is to elucidate the mechanism of chiral recognition by investigating the

* To whom all correspondence should be addressed.

• Abstract published in *Advance ACS Abstracts*, August 15, 1994.

0024-9297/94/2227-5821$04.50/0

relationship among *molecular*, *macromolecular*, and *supramolecular* structure and the extent of manifestation of heterochiral recognition in various liquid crystalline phases.

The main tool used in our studies consists of low molar mass mesogenic vinyl ethers and the corresponding homopolymers and copolymers prepared by living cationic polymerization. Living cationic polymerization produces polymers and copolymers with well-defined molecular weight, composition, narrow molecular weight distribution, and low chemical heterogeneity. Therefore, this technique is especially suitable for the synthesis of polymers used in chiral molecular recognition experiments.[6,7]

As a starting material for the synthesis of the chiral tail which is to be connected to the biphenylcarboxylate mesogen used in most of our investigations, we have chosen L- and/or D-α-amino acids. The reasons for this selection are as follows. The amino group of the α-amino acid can be substituted by fluorine,[8] chlorine,[9] and bromine[10b] atoms without affecting the original optical purity of the α-amino acid. The halogen atom introduced in the stereocenter provides a strong dipole moment in the chiral center and also creates a different steric environment around the chiral center which is determined by its size. Thus the halogen provides a useful probe which is necessary in the investigation of the mechanism responsible for chiral recognition. The steric hindrance in the chiral tail can be modified by changing the length and ramification of the alkyl chain of the α-amino acid. For this purpose, alanine, valine, leucine, and isoleucine are especially useful starting materials. Similar concepts based on the utilization of α-amino acids were used in the field of low molar mass chiral liquid crystals to elucidate the relationship between molecular structure and ferroelectric properties.[5b,c,10-12]

Prior to our first reports on interactions between the stereocenters of two enantiomeric side chain liquid crystalline polymers, there were cases in which strong complexes were observed between helical structures of *R* and *S* polymers.[13] However, in these cases stereocomplexation affects only crystalline phases and may not occur via chiral interactions but via interactions between left- and right-handed helical structures.

In the first publication of this series, we reported the observation of the first example of heterochiral recognition in the S_A phase of molecular pairs of diastereomeric liquid crystals based on (2*R*,3*S*)- and (2*S*,3*S*)-2-fluoro-3-methylpentyl 4′-((11-(vinyloxy)undecanyl)oxy)biphenyl-4-carboxylate.[14] This chiral recognition event was not detected in the corresponding polymers and copolymers. In the second publication, we reported the first example of the polymer effect on heterochiral recognition in molecular and macromolecular pairs of enantiomeric liquid crystals based on (*R*)- and (*S*)-2-chloro-4-methylpentyl 4′-((8-(vinyloxy)octyl)oxy)biphenyl-4-carboxylate.[15] For the first time, heterochiral molecular recognition was observed in the S_A phase but not in the S_C* phase of pairs of enantiomeric polymers. An influence of polymer molecular weight on chiral recognition was also observed. However, chiral recognition was not observed in copolymers.

The first goal of this paper is to describe the synthesis and the living cationic polymerization of (*R*)-2-fluoro-4-methylpentyl 4′-((8-(vinyloxy)octyl)oxy)biphenyl-4-carboxylate ((*R*)-**8**) and (*S*)-2-fluoro-4-methylpentyl 4′-((8-(vinyloxy)octyl)oxy)biphenyl-4-carboxylate ((*S*)-**8**) enantiomers. The presence of fluorine instead of chlorine in the chiral center of these compounds enhances the dipole moment of the stereocenter. The second goal of this paper is to compare the mesomorphic behavior of these two enantiomeric structural units and to investigate the heterochiral recognition in enantiomeric binary mixtures of monomers and of polymers, as well as in copolymers. To our knowledge, this paper will report the first example of heterochiral molecular recognition observed in the tilted S_C* phase of side chain liquid crystalline polymers and copolymers, and in the S_X phase of copolymers.

Experimental Section

Materials. L-Leucine ((*S*)-(+)-2-amino-4-methylpentanoic acid, 99%), D-leucine ((*R*)-(−)-2-amino-4-methylpentanoic acid, 99%), pyridinium poly(hydrogen fluoride) (HF 70% by weight), and borane–tetrahydrofuran complex (BH_3·THF, 1.0 M solution in THF) (all from Aldrich) were used as received.

Pyridine was heated overnight at 100 °C over KOH, distilled from KOH, and then stored over KOH. CH_2Cl_2 was refluxed over CaH_2 overnight and distilled from CaH_2. Dimethyl sulfoxide (DMSO) was heated overnight at 100 °C over CaH_2, distilled from CaH_2 under vacuum, and stored over molecular sieves, 4 Å. Tetrahydrofuran (THF) was refluxed over $LiAlH_4$ for several days and distilled from $LiAlH_4$. Acetone was stored over anhydrous K_2CO_3 for several days, filtered, and distilled.

CH_2Cl_2 used as a polymerization solvent was first washed with concentrated H_2SO_4 several times until the acid layer remained colorless and then washed with water, dried over $MgSO_4$, refluxed over CaH_2, and freshly distilled under argon before each use. Dimethyl sulfide ($(CH_3)_2S$) used in polymerizations (Aldrich, anhydrous, 99+%, packed under nitrogen in sure/seal bottle) was used as received. Trifluoromethanesulfonic acid (CF_3SO_3H) used as a polymerization initiator (Aldrich, 98%) was distilled under vacuum.

All other materials were commercially available and were used as received.

Techniques. ^{1}H-NMR spectra were recorded on a Varian XL-200 (200 MHz) spectrometer with TMS as the internal standard.

Relative molecular weights of polymers were determined by gel permeation chromatography (GPC). GPC analyses were carried out with a Perkin-Elmer Series 10LC instrument equipped with an LC-100 column oven and a Nelson Analytical 900 Series data station. Measurements were made by using a UV detector, THF as a solvent (1 mL/min, 40 °C), a set of PL gel columns of 5×10^2 and 10^4 Å, and a calibration plot constructed with polystyrene standards.

A Perkin-Elmer DSC-7 differential scanning calorimeter (DSC) was used to determine the thermal transition temperatures, which were reported as the maxima and minima of their endothermic or exothermic peaks respectively. Heating and cooling rates were 20 °C/min for the analysis of the homopolymers and 10 °C/min for the analysis of the monomer mixtures, polymer mixtures, and copolymers.

X-ray diffraction measurements were performed with a Rigaku powder diffractometer. The monochromatized X-ray beam from Cu Kα radiation with a wavelength of 0.154 18 nm was used. A temperature controller was added to the X-ray apparatus for thermal measurements. The precision of the controller was ±0.5 °C in the temperature range studied.

A Carl-Zeiss optical polarizing microscope equipped with a Mettler FP-82 hot stage and a Mettler FP-80 central processor was used to observe the thermal transitions and to analyze the anisotropic textures.

Synthesis of Monomers. Monomers (*R*)-**8** and (*S*)-**8** were synthesized from D-(*R*)-leucine and L-(*S*)-leucine, respectively, by following the synthetic route outlined in Scheme 1. The synthesis of compounds **5** and **7** were described previously.[7] This synthetic procedure will be described in detail only for monomer (*R*)-**8**.

(*R*)-2-Fluoro-4-methylpentanoic Acid ((*R*)-2).[8] Precooled (0 °C) dry pyridine (60 mL) was added dropwise to pyridinium poly(hydrogen fluoride) (HF 70% by weight, 100 g) in a Teflon flask at 0 °C. D-Leucine (10.5 g, 80.0 mmol) was dissolved in this solution, and $NaNO_2$ (8.28 g, 120.0 mmol) was added in six portions over a period of 1 h at 0 °C with vigorous stirring. The reaction mixture was allowed to warm to room temperature, and

Scheme 1. Synthesis of Monomers (*R*)-8 and (*S*)-8

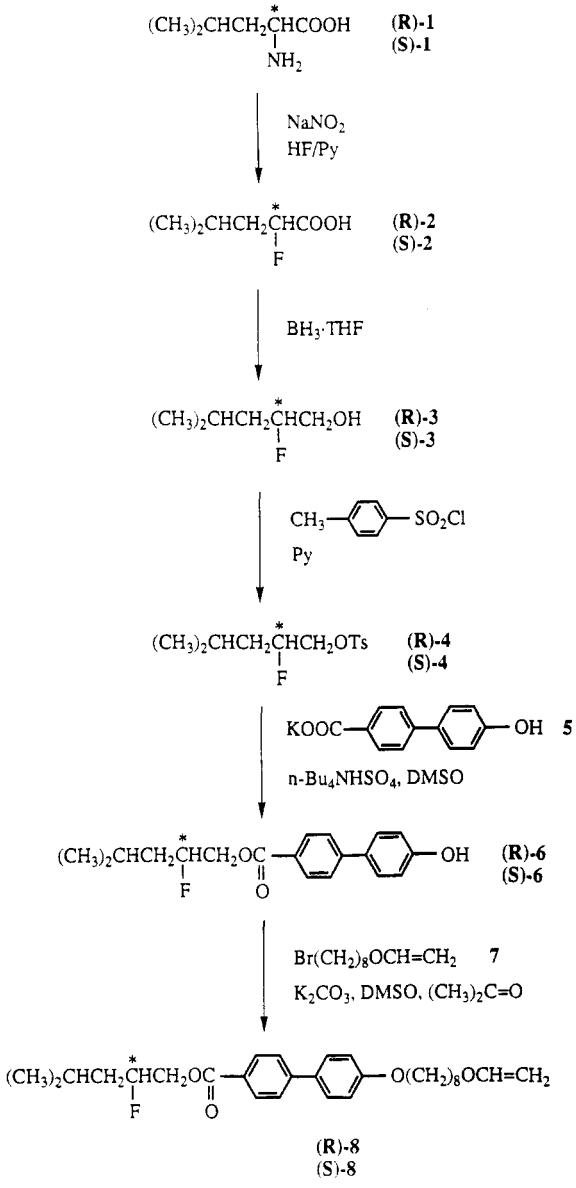

stirring was continued for 5 h. The mixture was poured into water, and the product was extracted into diethyl ether three times using a Teflon separatory funnel. The combined ethereal extracts were dried over anhydrous $MgSO_4$, and the solvent was evaporated to give a yellow crude product. The reaction was repeated at the same scale, and the crude products obtained from the two reactions were combined and distilled under vacuum to yield a colorless liquid (5.12 g, 23.9%). Bp: 60–75 °C (2.5 mmHg). ^{1}H-NMR ($CDCl_3$, TMS): δ 1.00 (d, J = 6.1 Hz, 6H, $(CH_3)_2CH$—), 1.75–2.13 (m, 3H, $(CH_3)_2CHCH_2$—), 5.00 (ddd, J = 49.5, 9.2, and 3.4 Hz, 1H, —CHF—), 10.6 (bs, 1H, —COOH).

(*R*)-2-Fluoro-4-methylpentanol ((*R*)-3). A solution of borane–THF complex in THF (1.0 M, 36.7 mL, 36.7 mmol) was added dropwise to a stirred, cooled (0 °C) solution of compound (*R*)-2 (4.10 g, 30.6 mmol) in dry THF (80 mL) over 1 h under a nitrogen atmosphere. The reaction mixture was allowed to warm to room temperature, and stirring was continued for 2 h. Then the reaction mixture was cooled to 0 °C again, and 4 mL of water followed by 80 mL of saturated K_2CO_3 solution was added. The product was extracted into diethyl ether twice, and the combined organic layers were dried over anhydrous $MgSO_4$. The solvent was evaporated and the remaining crude product (3.48 g, 94.6%) was used for the synthesis of (*R*)-4 without further purification. ^{1}H-NMR ($CDCl_3$, TMS): δ 0.96 (d, J = 6.4 Hz, 6H, $(CH_3)_2CH$—), 1.47–1.98 (m, 3H, $(CH_3)_2CHCH_2$—), 2.28 (bs, 1H, —CH_2OH), 3.55–3.79 (m, 2H, —CH_2OH), 4.47–4.63, 4.72–4.88 (dm, J = 50.0 Hz, 1H, —CHF—).

(*R*)-2-Fluoro-4-methylpentyl Tosylate ((*R*)-4). A solution of compound (*R*)-3 (3.48 g, 29.0 mmol, crude) in dry pyridine (10 mL) was added dropwise to a stirred, cooled (0 °C) solution of *p*-toluenesulfonyl chloride (8.28 g, 43.4 mmol) in dry pyridine (50 mL). The mixture was allowed to warm to room temperature and stirred overnight. The mixture was poured into water, and the product was extracted into diethyl ether twice. The combined ethereal extracts were washed with 10% HCl twice and dried over anhydrous $MgSO_4$. The solvent was evaporated and the remaining crude product was purified by column chromatography (silica gel; hexane–ethyl acetate 15:1) to give a colorless liquid (5.60 g, 72.3%). Purity: >99% (TLC). ^{1}H-NMR ($CDCl_3$, TMS): δ 0.91, 0.92 (d, J = 6.5 Hz, 6H, $(CH_3)_2CH$—), 1.09–1.46 (m, 1H, $(CH_3)_2CH$—), 1.46–1.93 (m, 2H, $(CH_3)_2CHCH_2$—), 2.46 (s, 3H, —PhCH_3), 3.98–4.20 (m, 2H, —CH_2OSO_2—), 4.52–4.67, 4.76–4.91 (dm, J = 52.7 Hz, 1H, —CHF—), 7.37 (d, J = 8.2 Hz, 2ArH, ortho to —CH_3), 7.81 (d, J = 8.2 Hz, 2ArH, ortho to —SO_2—).

(*R*)-2-Fluoro-4-methylpentyl 4′-Hydroxybiphenyl-4-carboxylate ((*R*)-6). A mixture of (*R*)-4 (5.60 g, 20.4 mmol), 5 (5.15 g, 20.4 mmol), tetrabutylammonium hydrogen sulfate (TBAH, 1.02 g), and dry DMSO (50 mL) was stirred at 80 °C under a nitrogen atmosphere for 20 h. The resulting clear yellow solution was poured into water. The product was extracted into diethyl ether twice, and the combined ethereal extracts were dried over anhydrous $MgSO_4$. The solvent was evaporated and the remaining crude product was purified by column chromatography (silica gel; hexane–ethyl acetate 3:1) to give a colorless solid which was recrystallized from hexane–ethyl acetate (13:1) to yield colorless crystals (4.47 g, 69.3%). Purity: >99% (TLC). Mp: 91.3 °C (DSC, 20 °C/min). ^{1}H-NMR ($CDCl_3$, TMS): δ 0.99 (d, J = 6.3 Hz, 6H, $(CH_3)_2CH$—), 1.24–1.59 (m, 1H, $(CH_3)_2CH$—), 1.64–2.00 (m, 2H, $(CH_3)_2$—$CHCH_2$—), 4.27–4.62 (m, 2H, —CH_2OCO—), 4.71–4.86, 4.95–5.11 (dm, J = 50.4 Hz, 1H, —CHF—), 5.79 (bs, 1H, —PhO*H*), 6.96 (d, J = 8.5 Hz, 2ArH, ortho to —OH), 7.52 (d, J = 8.5 Hz, 2ArH, meta to —OH), 7.62 (d, J = 8.3 Hz, 2ArH, meta to —COO—), 8.12 (d, J = 8.3 Hz, 2ArH, ortho to —COO—).

(*R*)-2-Fluoro-4-methylpentyl 4′-((8-(Vinyloxy)octyl)oxy)-biphenyl-4-carboxylate ((*R*)-8). A mixture of compound (*R*)-6 (3.53 g, 11.2 mmol), anhydrous K_2CO_3 (3.87 g, 28.0 mmol), and acetone (90 mL) was stirred at 60 °C under a nitrogen atmosphere for 2 h. To the resulting yellow solution was added a solution of 7 (2.62 g, 11.2 mmol) in dry DMSO (5.0 mL), and stirring was continued at 60 °C for 20 h. The mixture was poured into water, and the product was extracted into diethyl ether twice. The combined ethereal extracts were dried over anhydrous $MgSO_4$. The solvent was evaporated and the remaining crude product was purified by column chromatography twice (silica gel; hexane–ethyl acetate 20:1) to yield a white solid (2.47 g, 46.9%). Purity: >99% (TLC). The thermal transition temperatures are given in Table 3. ^{1}H-NMR ($CDCl_3$, TMS): δ 0.99 (d, J = 6.2 Hz, 6H, $(CH_3)_2CH$—), 1.22–1.98 (m, 15H, $(CH_3)_2CHCH_2$—, CH_2=$CHOCH_2(CH_2)_6CH_2O$—), 3.68 (t, J = 6.5 Hz, 2H, CH_2=CH—OCH_2—), 3.98 (dd, J = 6.9 and 1.6 Hz, 1H, CH_2=CHO— trans), 4.01 (t, J = 6.5 Hz, 2H, —CH_2OPh—), 4.17 (dd, J = 14.3 and 1.6 Hz, 1H, CH_2=CHO— cis), 4.27–4.61 (m, 2H, —CH_2-OCO—), 4.71–4.87, 4.96–5.10 (dm, J = 50.1 Hz, 1H, —CHF—), 6.48 (dd, J = 14.3 and 6.9 Hz, 1H, CH_2=CHO—), 7.00 (d, J = 8.6 Hz, 2ArH, ortho to —$(CH_2)_8O$—), 7.58 (d, J = 8.6 Hz, 2ArH, meta to —$(CH_2)_8O$—), 7.64 (d, J = 8.4 Hz, 2ArH, meta to —COO—), 8.12 (d, J = 8.4 Hz, 2ArH, ortho to —COO—).

Cationic Polymerizations. Polymerizations and copolymerizations were carried out in a three-necked round bottom flask equipped with a Teflon stopcock and rubber septa under argon atmosphere at 0 °C for 1 h. All glassware was dried overnight at 140 °C. The monomer was further dried under vacuum overnight in the polymerization flask. After the flask was filled with argon, freshly distilled dry methylene chloride was added via a syringe and the solution was cooled to 0 °C. $(CH_3)_2S$ and CF_3SO_3H were then added carefully via a syringe. The monomer concentration was about 0.224 M, and the $(CH_3)_2S$ concentration was 10 times larger than that of CF_3SO_3H. The polymer molecular weight was controlled by the monomer/initiator ($[M]_o/[I]_o$) ratio. After quenching the polymerization with a mixture of NH_4OH and methanol (1:2), the reaction mixture was poured into methanol to give a white precipitate.

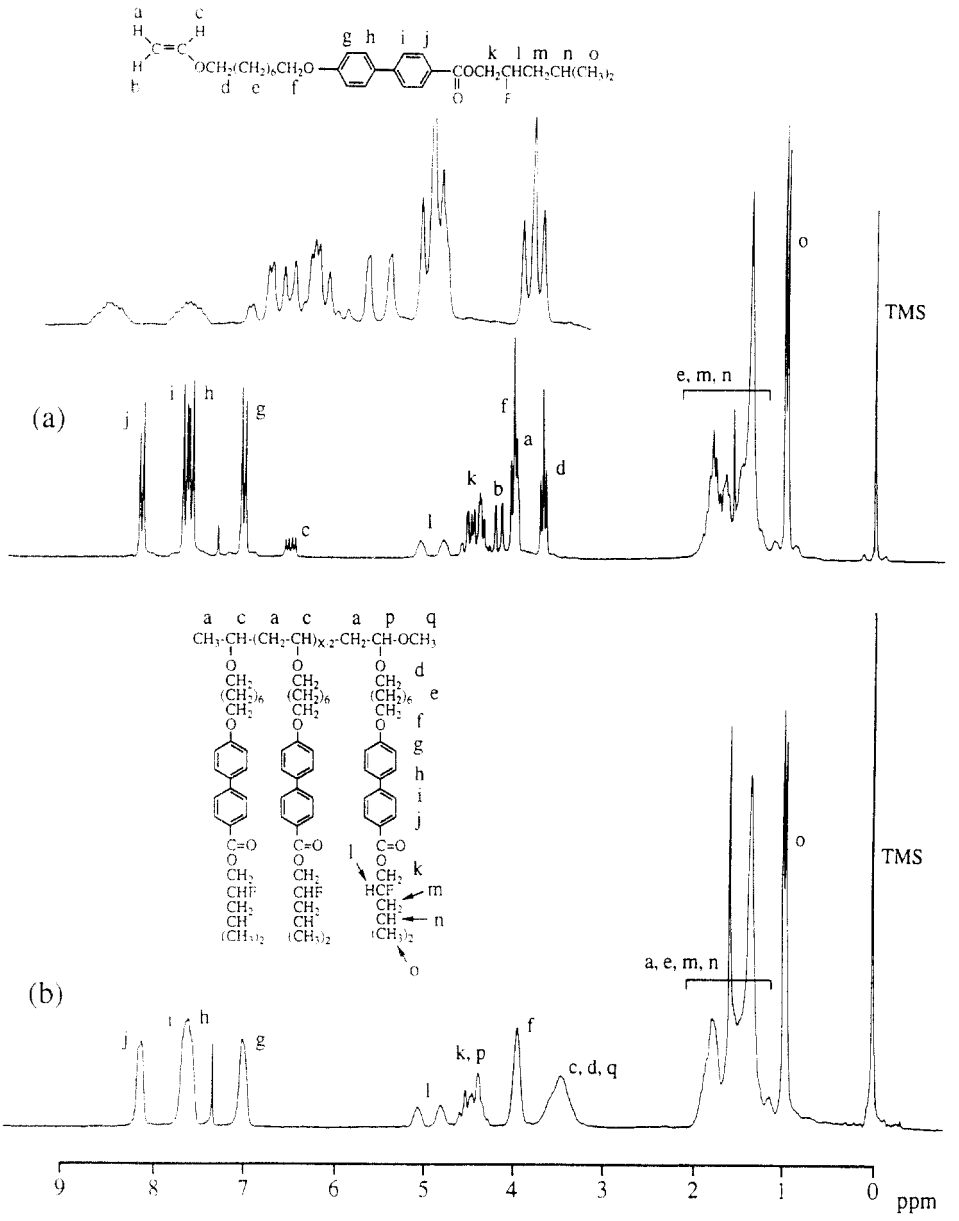

Figure 1. ^{1}H-NMR spectra of monomer (*R*)-8 (a) and polymer poly[(*R*)-8] (DP = 9.3) (b).

The obtained polymer was purified by reprecipitation by pouring its chloroform solution into methanol and dried under vacuum.

Results and Discussion

Determination of the Optical Purities of Monomers (*R*)-8 and (*S*)-8. The synthesis of two enantiomeric monomers (*R*)- and (*S*)-8 is outlined in Scheme 1. Monomers (*R*)-8 and (*S*)-8 were synthesized from D-(*R*)-leucine and L-(*S*)-leucine, respectively, in the same manner. The amino groups of D-(*R*)- and L-(*S*)-leucine were substituted with a fluorine atom via a diazonium salt by using $NaNO_2$ in a HF–pyridine complex.[8] Since this reaction proceeds with the retention of configuration at the chiral center, the original configurations of D-(*R*)- and L-(*S*)-leucine are maintained throughout the entire steps of the synthesis. The reduction of the carboxyl groups of compounds (*R*)- and (*S*)-2 was carried out with a BH_3·THF complex without affecting the fluorine atom of the chiral center. Reduction experiments with $LiAlH_4$ showed that it reduces the fluorine atom, resulting in the partial loss of the chiral center.

The optical purities of monomers (*R*)- and (*S*)-8 and of the corresponding polymers poly[(*R*)-8] and poly[(*S*)-8] were investigated by the NMR chiral shift reagent technique described by Goodby et al.[5b,16] The chiral shift reagent used in this study was a tris[3-(heptafluoropropylhydroxymethylene)-(+)-camphorato]europium(III) derivative (Eu(hfc)$_3$). Figure 1 presents the ^{1}H-NMR spectra of monomer (*R*)-8 and polymer poly[(*R*)-8] (DP = 9.3), both spectra without Eu(hfc)$_3$. No change in the resonances of the protons attached to the chiral center are observed after polymerization. Figure 2a presents the ^{1}H-NMR spectrum of the 50/50 mixture between (*R*)- and (*S*)-8 with Eu(hfc)$_3$ [(*R*)-8 5 mg, (*S*)-8 5 mg, and Eu(hfc)$_3$ 10 mg]. The ^{1}H-NMR spectra of pure (*R*)- and (*S*)-8 with Eu(hfc)$_3$ [monomer 10 mg and Eu(hfc)$_3$ 10 mg] are presented in Figure 2b,c, respectively. The assignment of all resonances is printed on these figures. They are self-explanatory and will not be discussed here. As shown in Figure 2, the doublet associated with the aromatic proton j which is adjacent to the chiral center is split in the 50/50 mixture of the monomers, while the corresponding peaks remained unchanged in pure (*R*)-8 and (*S*)-8 except that they were shifted downfield. When the amount of the shift reagent was increased, a broadening of the peaks was observed before the complete separation of the two doublets was achieved and, therefore, it was difficult to calculated the optical purities of both monomers precisely.

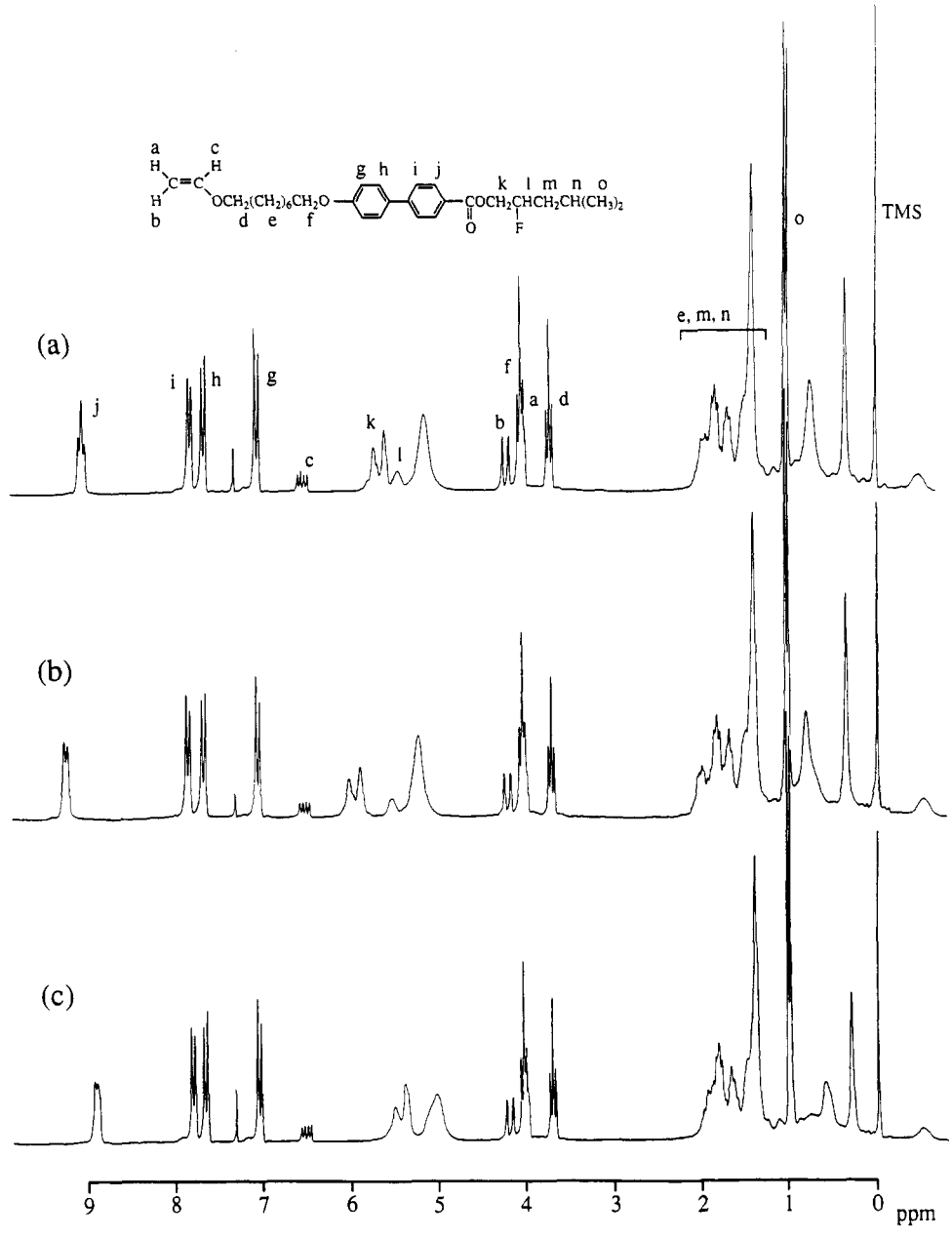

Figure 2. ^{1}H-NMR spectra of the monomer mixture and monomers with Eu(hfc)$_3$: (a) (*R*)-8/(*S*)-8 (50/50 mixture); (b) (*R*)-8; (c) (*S*)-8.

Judging from Figure 2b,c, it seems that no racemization has occurred throughout the synthesis of the monomers and their optical purities are expected to be higher than 95%. The same technique was also applied to polymers. The polymers showed broadened peaks even in the absence of the shift reagent (Figure 1b), and this made the separation of the peaks impossible. However, if we compare Figures 1 and 2, it becomes clear that the chiral center of the monomers is insensitive to the cationic polymerization conditions and, therefore, the original optical purities of the monomers remain unchanged during this polymerization process. This was the case in previous examples of cationic polymerization of similar chiral monomers with the same initiating system.[7,14,15]

Homopolymerization of (*R*)-8 and (*S*)-8. The homopolymerizations of (*R*)-8 and (*S*)-8 were carried out at 0 °C in CH_2Cl_2 by a living cationic polymerization technique using $CF_3SO_3H/(CH_3)_2S$ as the initiating system. Previous work in our laboratory[17] and others[18] has shown that the CF_3SO_3H initiated polymerization of vinyl ethers in the presence of a Lewis base such as $(CH_3)_2S$ produces well-defined polymers with controlled molecular weights and narrow polydispersities. The polymerization mechanism was discussed in detail in previous publications.[17,18]

The characterization results of poly[(*R*)-8] and poly[(*S*)-8] obtained by gel permeation chromatography (GPC) and differential scanning calorimetry (DSC) are summarized in Tables 1 and 2, respectively. The low yields are the result of the loss of polymer during purification. Relative number-average molecular weights of polymers determined by GPC exhibit a linear dependence on the initial molar ratio of monomer to initiator ($[M]_o/[I]_o$). All polydispersities are lower than 1.33. This slightly large polydispersity is probably due to the presence of a trace amount of moisture in the polymerization system. However, the $[M]_o/[I]_o$ ratio provides a good control of the polymer molecular weight. All these features demonstrate the typical characteristics of a living polymerization mechanism. The absolute number-average molecular weights were difficult to determine by ^{1}H-NMR spectroscopy from the chain ends[17c] of the polymer owing to signal overlap (see Figure 1b, signals q and a).

The phase behavior of poly[(*R*)-8] and poly[(*S*)-8] was characterized by a combination of techniques consisting

Table 1. Cationic Polymerization of (*R*)-2-Fluoro-4-methylpentyl 4'-((8-(Vinyloxy)octyl)oxy)biphenyl-4-carboxylate ((*R*)-8) and Characterization of the Resulting Polymers[a]

sample no.	$[M]_o/[I]_o$	polymer yield (%)	$10^{-3}M_n$	M_w/M_n	DP	phase transitions (°C) and corresponding enthalpy changes (kcal/mru) heating	cooling
1	3	24.6	1.93	1.13	4.1	K 49.6 (1.18) S_C^* 91.7 (1.52) I	I 84.1 (−1.65) S_C^* 34.1 (−0.90) K
2	8	63.1	2.64	1.22	5.6	K 61.1 (1.39) S_C^* 96.1 (1.55) I	I 87.6 (−1.58) S_C^* 45.0 (−1.15) K
3	12	75.4	4.36	1.28	9.3	K 75.3 (1.39) S_C^* 107.3 (1.52) I	I 98.2 (−1.58) S_C^* 69.4 (†[b]) S_X 60.4 (−1.25) K
4	16	62.7	5.50	1.13	11.7	K 77.7 (1.13) S_X 83.1 (0.15) S_C^* 110.9 (1.48) I	I 102.1 (−1.52) S_C^* 76.3 (−0.12) S_X 63.9 (−0.75) K
5	20	78.5	6.21	1.11	13.2	K 83.1 (1.14) S_X 91.3 (0.20) S_C^* 113.6 (1.50) I	I 105.0 (−1.50) S_C^* 84.6 (−0.16) S_X 68.3 (−0.73) K
6	30	74.5	7.66	1.14	16.3	K 82.3 (1.07) S_X 94.2 (0.24) S_C^* 115.7 (1.46) I	I 106.5 (−1.50) S_C^* 87.2 (−0.17) S_X 68.3 (−0.79) K

[a] Conditions: polymerization temperature, 0 °C; polymerization solvent, methylene chloride $[M]_o = 0.224$; $[Me_2S]_o/[I]_o = 10$; polymerization time, 1 h. Data are from second heating and first cooling scans. (Heating and cooling rates are 20 °C/min.) [b] Overlapped peaks.

Table 2. Cationic Polymerization of (*S*)-2-Fluoro-4-methylpentyl 4'-((8-(Vinyloxy)octyl)oxy)biphenyl-4-carboxylate ((*S*)-8) and Characterization of the Resulting Polymers[a]

sample no.	$[M]_o/[I]_o$	polymer yield (%)	$10^{-3}M_n$	M_w/M_n	DP	phase transitions (°C) and corresponding enthalpy changes (kcal/mru) heating	cooling
1	5	52.1	2.41	1.20	5.1	K 53.4 (1.18) S_C^* 93.4 (1.50) I	I 84.8 (−1.62) S_C^* 38.5 (−0.94) K
2	8	60.4	2.74	1.29	5.8	K 61.0 (1.23) S_C^* 99.5 (1.49) I	I 91.2 (−1.66) S_C^* 47.2 (−1.13) K
3	12	71.2	3.04	1.33	6.5	K 68.2 (1.43) S_C^* 101.0 (1.55) I	I 92.3 (−1.56) S_C^* 53.0 (−1.21) K
4	16	73.2	5.00	1.11	10.6	K 74.7 (1.29) S_C^* 107.5 (1.48) I	I 98.7 (−1.52) S_C^* 68.3 (†[b]) S_X 60.7 (−1.11) K
5	20	75.7	5.94	1.11	12.6	K 77.4 (1.06) S_X 84.5 (0.18) S_C^* 111.3 (1.50) I	I 102.3 (−1.51) S_C^* 77.3 (−0.12) S_X 64.0 (−0.73) K
6	30	75.5	7.14	1.15	15.2	K 82.1 (1.10) S_X 93.0 (0.23) S_C^* 115.0 (1.48) I	I 104.9 (−1.50) S_C^* 84.8 (−0.17) S_X 66.9 (−0.76) K

[a] Reaction conditions and characterization data are as in Table 1. [b] Overlapped peak.

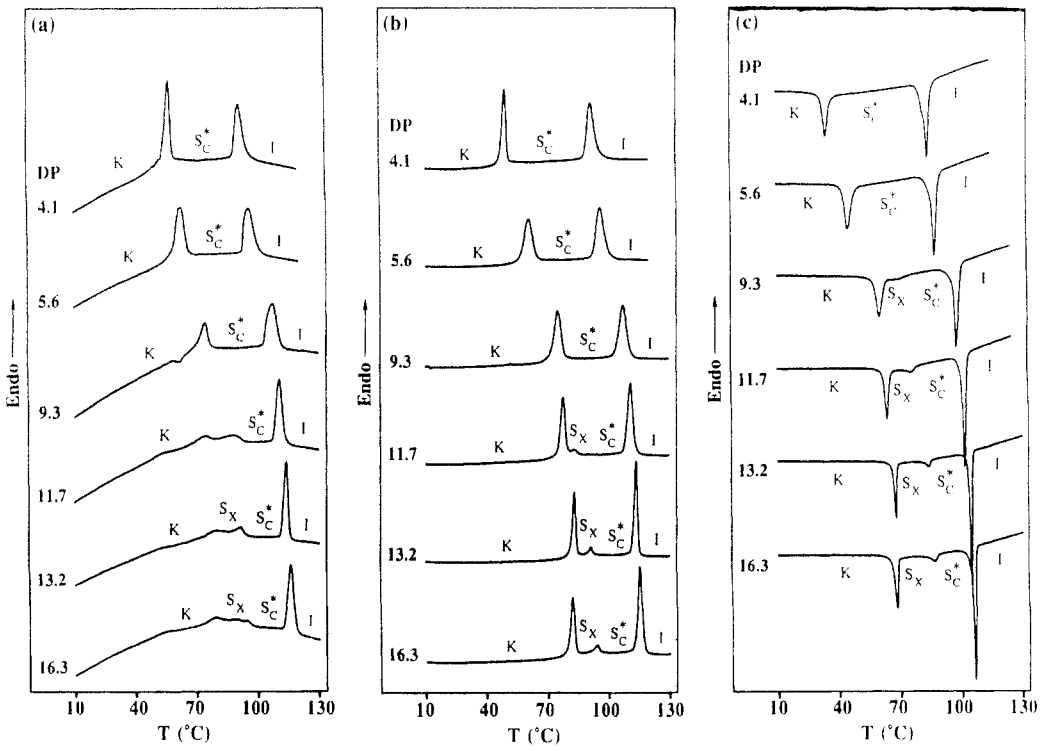

Figure 3. DSC thermograms (20 °C/min) of poly[(*R*)-8] with different DP: (a) first heating scans; (b) second heating scans; (c) first cooling scans.

of DSC, thermal optical polarized microscopy, and X-ray diffraction. Figure 3 presents the DSC thermograms of poly[(*R*)-8] and poly[(*S*)-8] at identical molecular weights with various degrees of polymerization (DP). The DSC thermograms of poly[(*S*)-8] are identical to those of poly-[(*R*)-8] and are not shown. The phase behaviors of the two enantiomeric homopolymers can be compared by superimposing the plots of the dependencies of their thermal transition temperatures as a function of DP (Figure 4). As observed from this figure, the phase behavior of poly[(*R*)-8] is identical to that of poly[(*S*)-8]. All polymers are crystalline and exhibit an enantiotropic S_C^* phase above their melting temperature (see X-ray and optical polarized microscopy discussions). Polymers with DP > 11 show an additional unidentified smectic (S_X) phase between the crystalline and S_C^* phases. It is interesting to observe that poly[(*R*)-8] and poly[(*S*)-8] do not display a S_A mesophase. Even when DSC experiments were performed at lower heating and cooling rates (<10 °C/min), the transition peak between the S_C^* and isotropic phases did not split into two peaks and, therefore, no evidence for the existence of a S_A phase was obtained. A

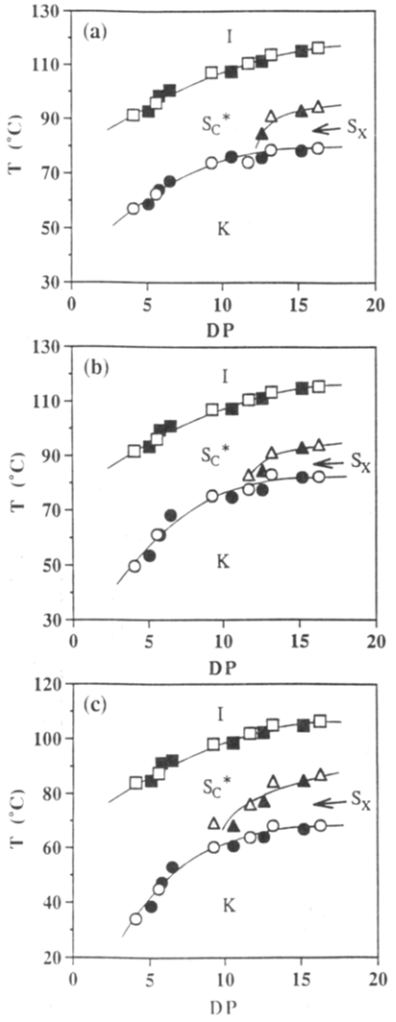

Figure 4. Dependence of phase transition temperatures on the degree of polymerization of poly[(*R*)-8] (open) and poly[(*S*)-8] (closed): (a) data from the first heating scans; (b) data from the second heating scans; (c) data from the first cooling scans.

similar example in which an enantiotropic S_C* phase directly melts into and forms from an isotropic phase was reported in a previous publication from our laboratory.[7d] Representative optical polarized micrographs of the textures exhibited by the S_C* and S_X phases of poly[(*S*)-8] (DP = 15.2) are presented in Figure 5.

In order to confirm the assignment of the S_C* mesophase, X-ray diffraction measurements were carried out. Figure 6 presents the temperature dependence of the layer spacing obtained from poly[(*S*)-8] (DP = 12.6). Measurements were performed on the second heating scan, and the scanning rates were 1.25 and 10 °C/min. The layer spacing is almost constant below 80 °C and decreases drastically between 80 and 85 °C. These temperatures are in good agreement with the S_X–S_C* transition temperature determined by the DSC analysis (84.5 °C, 10 °C/min). The layer spacing below 80 °C is 27.1 Å, and this value is identical to the calculated side chain length of the structural unit of the polymer. Above 85 °C, the layer spacing increases linearly with increasing temperature and disappears at the isotropization temperature before recovering to the original constant value (27.1 Å). These results clearly demonstrate the presence of a tilted (S_C*) phase and the absence of an untilted (S_A) phase.

Miscibility Studies. Monomer (*R*)-8 and monomer (*S*)-8 were mixed in various compositions, and their phase behavior was investigated by DSC. Mixtures were prepared by dissolving the two monomers in CH_2Cl_2 followed by evaporation of the solvent under vacuum. Four sets of binary mixtures between poly[(*R*)-8] and poly[(*S*)-8] with different molecular weights were also prepared and their phase behavior was investigated in the same manner. The molecular weights and polydispersities of the polymers employed in this miscibility study are as follows: polymer mixture I poly[(*R*)-8] with DP = 5.6, M_w/M_n = 1.22 and poly[(*S*)-8] with DP = 5.1, M_w/M_n = 1.20; polymer mixture II poly[(*R*)-8] with DP = 11.7, M_w/M_n = 1.13 and poly[(*S*)-8] with DP = 10.6, M_w/M_n = 1.11; polymer mixture III poly[(*R*)-8] with DP = 13.2, M_w/M_n = 1.11 and poly[(*S*)-8] with DP = 13.1, M_w/M_n = 1.15; polymer mixture

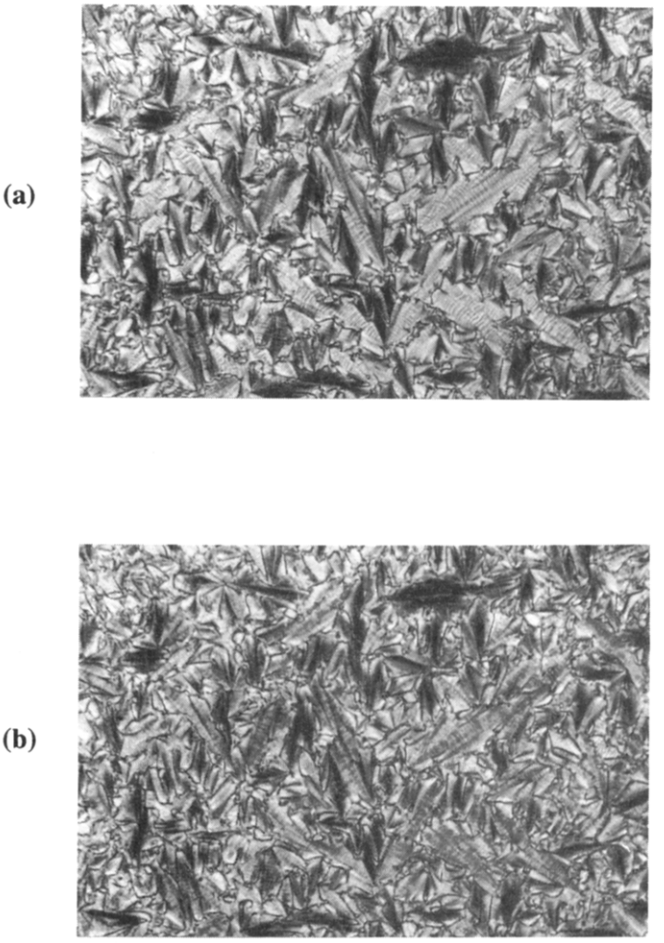

Figure 5. Representative optical micrographs of the S_C* mesophase displayed by poly[(*S*)-8] (DP = 15.2) upon heating to 100 °C (a) and the S_X mesophase displayed by poly[(*S*)-8] (DP = 15.2) upon cooling to 91 °C (b).

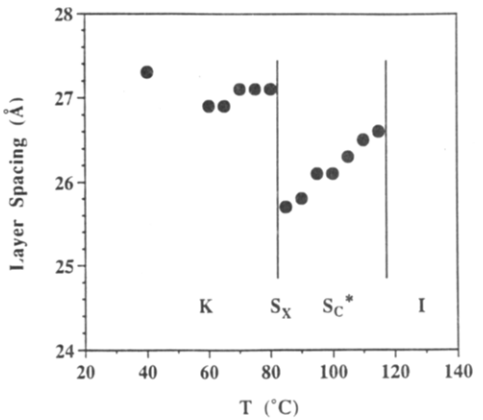

Figure 6. Temperature dependence of the layer spacing of poly[(*S*)-8] (DP = 12.6).

Table 3. Characterization of the Binary Mixtures of Monomers (*R*)-8 with (*S*)-8[a]

(*R*)-8/(*S*)-8 (mol/mol)	phase transitions (°C) and corresponding enthalpy changes (kcal/mol)	
	heating	cooling
0/100	K 28.7 (−0.46) K 38.2 (4.51) S_C* 47.2 (0.05) S_A 60.5 (1.51) I	I 56.8 (−1.51) S_A 44.0 (−0.07) S_C* 4.7 (−0.05) S_X 0.8 (−2.38) K
11.4/88.6	K 29.3 (−0.99) K 39.9 (5.51) S_C* 46.9 (0.04) S_A 60.7 (1.52) I	I 56.9 (−1.52) S_A 43.8 (−0.07) S_C* 3.0 (†[b]) S_X −1.1 (−2.76) K
20.4/79.6	K 27.5 (−1.09) K 41.0 (5.61) S_C* 46.8 (0.03) S_A 60.9 (1.53) I	I 56.9 (−1.54) S_A 43.5 (−0.05) S_C* 1.9 (†[b]) S_X −1.3 (−2.76) K
39.9/60.1	K 28.7 (−1.51) K 41.8 (5.61) S_C* 46.4 (0.02) S_A 60.9 (1.52) I	I 57.1 (−1.53) S_A 43.1 (−0.06) S_C* −1.2 (−2.73) K
45.1/54.9	K 28.8 (−1.08) K 41.8 (5.67) S_C* 46.4 (0.02) S_A 60.9 (1.50) I	I 57.2 (−1.50) S_A 43.2 (−0.06) S_C* −1.1 (−2.68) K
50.1/49.9	K 28.7 (−1.24) K 41.9 (5.65) S_C* 46.4 (†[b]) S_A 61.0 (1.52) I	I 57.1 (−1.53) S_A 43.0 (−0.06) S_C* −1.2 (−2.71) K
54.0/46.0	K 28.9 (−1.42) K 41.8 (5.47) S_C* 46.4 (0.02) S_A 61.0 (1.48) I	I 57.2 (−1.49) S_A 43.1 (−0.06) S_C* −1.2 (−2.63) K
59.4/40.6	K 28.9 (−1.07) K 41.9 (5.67) S_C* 46.5 (0.01) S_A 61.1 (1.51) I	I 57.2 (−1.53) S_A 43.3 (−0.05) S_C* −1.1 (−2.67) K
78.2/21.8	K 27.2 (−1.14) K 40.7 (5.53) S_C* 46.7 (0.02) S_A 60.9 (1.52) I	I 57.1 (−1.53) S_A 43.5 (−0.06) S_C* 1.9 (†[b]) S_X −1.5 (−2.71) K
88.9/11.1	K 29.3 (−0.94) K 39.8 (5.38) S_C* 46.9 (0.05) S_A 60.8 (1.49) I	I 56.9 (−1.53) S_A 43.5 (−0.07) S_C* 3.0 (−0.04) S_X −1.5 (−2.61) K
100/0	K 28.2 (−0.38) K 38.0 (4.54) S_C* 47.1 (0.05) S_A 60.6 (1.51) I	I 56.8 (−1.53) S_A 44.1 (−0.07) S_C* 4.8 (−0.05) S_X 0.3 (−2.44) K

[a] Data are from second heating and first cooling scans (10 °C/min). [b] Overlapped peak.

Table 4. Characterization of the Binary Mixtures of Poly[(*R*)-8] (DP = 5.6, M_w/M_n = 1.22) with Poly[(*S*)-8] (DP = 5.1, M_w/M_n = 1.20) (Polymer Mixture I)[a]

poly[(*R*)-8]/poly[(*S*)-8] (mol/mol)	phase transitions (°C) and corresponding enthalpy changes (kcal/mru)	
	heating	cooling
0/100	K 52.7 (1.34) S_C* 91.9 (1.61) I	I 87.8 (−1.65) S_C* 41.6 (−1.12) K
12.2/87.8	K 52.2 (1.30) S_C* 92.6 (1.59) I	I 88.3 (−1.63) S_C* 41.6 (−1.06) K
21.7/78.3	K 52.0 (1.25) S_C* 92.9 (1.57) I	I 88.7 (−1.63) S_C* 41.8 (−1.08) K
39.5/60.5	K 52.7 (1.24) S_C* 93.6 (1.58) I	I 89.5 (−1.63) S_C* 42.7 (−1.01) K
50.2/49.8	K 53.3 (1.23) S_C* 94.0 (1.61) I	I 89.6 (−1.63) S_C* 43.1 (−1.07) K
59.2/40.8	K 54.8 (1.30) S_C* 94.6 (1.60) I	I 90.0 (−1.68) S_C* 44.0 (−1.09) K
78.7/21.3	K 57.5 (1.40) S_C* 94.8 (1.61) I	I 90.1 (−1.68) S_C* 45.5 (−1.16) K
90.4/9.6	K 59.5 (1.39) S_C* 94.8 (1.52) I	I 90.6 (−1.65) S_C* 47.1 (−1.20) K
100/0	K 61.2 (1.55) S_C* 95.2 (1.62) I	I 90.7 (−1.68) S_C* 48.2 (−1.28) K

[a] Data are from second heating and first cooling scans (10 °C/min).

Table 5. Characterization of the Binary Mixtures of Poly[(*R*)-8] (DP = 11.7, M_w/M_n = 1.13) with Poly[(*S*)-8] (DP = 10.6, M_w/M_n = 1.11) (Polymer Mixture II)

poly[(*R*)-8]/poly[(*S*)-8] (mol/mol)	phase transitions (°C) and corresponding enthalpy changes (kcal/mru)	
	heating	cooling
0/100	K 73.6 (1.40) S_C* 105.6 (1.50) I	I 100.5 (−1.56) S_C* 69.8 (†[a]) S_X 62.5 (−1.22) K
11.3/88.7	K 72.8 (1.36) S_C* 106.0 (1.53) I	I 100.9 (−1.55) S_C* 70.9 (†[a]) S_X 62.4 (−1.21) K
21.3/78.7	K 72.3 (1.29) S_C* 106.4 (1.49) I	I 101.4 (−1.57) S_C* 71.5 (†[a]) S_X 62.5 (−1.22) K
39.1/60.9	K 71.8 (1.25) S_C* 107.1 (1.52) I	I 102.1 (−1.58) S_C* 73.1 (†[a]) S_X 62.7 (−1.23) K
50.2/49.8	K 71.7 (1.23) S_C* 107.3 (1.49) I	I 102.3 (−1.59) S_C* 73.1 (†[a]) S_X 62.8 (−1.30) K
59.1/40.9	K 72.3 (1.21) S_C* 107.7 (1.41) I	I 102.7 (−1.52) S_C* 73.4 (†[a]) S_X 63.3 (−1.15) K
78.1/21.9	K 73.7 (1.25) S_C 78.5 (†[a]) S_C* 108.2 (1.49) I	I 103.3 (−1.52) S_C* 75.8 (†[a]) S_X 64.3 (−1.35) K
89.2/10.8	K 75.2 (1.31) S_X 80.4 (†[a]) S_C* 108.6 (1.45) I	I 103.7 (−1.55) S_C* 76.0 (†[a]) S_X 64.9 (−1.34) K
100/0	K 76.4 (1.35) S_X 80.1 (†[a]) S_C* 108.9 (1.44) I	I 103.8 (−1.53) S_C* 76.9 (−0.25) S_X 65.5 (−1.00) K

[a] Overlapped peak.

Table 6. Characterization of the Binary Mixtures of Poly[(*R*)-8] (DP = 13.2, M_w/M_n = 1.11) with Poly[(*S*)-8] (DP = 13.1, M_w/M_n = 1.15) (Polymer Mixture III)[a]

poly[(*R*)-8]/poly[(*S*)-8] (mol/mol)	phase transitions (°C) and corresponding enthalpy changes (kcal/mru)	
	heating	cooling
0/100	K 79.9 (1.14) S_X 87.0 (0.18) S_C* 110.6 (1.49) I	I 105.8 (−1.52) S_C* 83.8 (−0.13) S_X 68.6 (−0.80) K
9.7/90.3	K 79.2 (1.13) S_X 87.1 (0.18) S_C* 110.9 (1.47) I	I 106.0 (−1.54) S_C* 83.8 (−0.13) S_X 68.4 (−0.76) K
20.4/79.6	K 78.7 (1.09) S_X 86.8 (0.19) S_C* 111.0 (1.46) I	I 106.3 (−1.54) S_C* 84.1 (−0.11) S_X 68.4 (−0.76) K
40.2/59.8	K 78.5 (1.09) S_X 87.0 (0.20) S_C* 111.5 (1.49) I	I 106.5 (−1.51) S_C* 84.1 (−0.11) S_X 68.3 (−0.75) K
50.2/49.8	K 78.4 (1.13) S_X 86.8 (0.21) S_C* 111.4 (1.49) I	I 106.7 (−1.51) S_C* 83.9 (−0.13) S_X 68.5 (−0.76) K
59.2/40.8	K 78.7 (1.13) S_X 87.4 (0.19) S_C* 111.6 (1.48) I	I 106.8 (−1.54) S_C* 84.4 (−0.16) S_X 68.6 (−0.79) K
79.3/20.7	K 80.0 (1.15) S_X 88.2 (0.19) S_C* 111.8 (1.47) I	I 107.0 (−1.52) S_C* 85.1 (−0.15) S_X 69.3 (−0.77) K
89.8/10.2	K 80.9 (1.21) S_X 89.0 (0.19) S_C* 111.9 (1.49) I	I 107.1 (−1.53) S_C* 85.7 (−0.13) S_X 69.8 (−0.75) K
100/0	K 82.0 (1.21) S_X 89.4 (0.18) S_C* 111.9 (1.43) I	I 107.3 (−1.51) S_C* 86.2 (−0.13) S_X 70.3 (−0.73) K

[a] Data are from second heating and first cooling scans (10 °C/min).

IV poly[(*R*)-8] with DP = 16.3, M_w/M_n = 1.14 and poly[(*S*)-8] with DP = 15.2, M_w/M_n = 1.15. The thermal transition temperatures and the corresponding enthalpy changes are summarized in Table 3 (for the monomer mixtures) and Tables 4–7 (for the polymer mixtures). The DSC thermograms of the monomer mixtures are presented in Figure 7. The phase diagrams of the monomer mixtures are plotted in Figure 8, and the phase diagrams of the polymer mixtures are presented in Figure 9.

The phase behavior of monomer (*R*)-8 is identical to that of monomer (*S*)-8. Both monomers display enantiotropic S_A and S_C*, a monotropic S_X, and a crystalline phase. When the two monomers are mixed, the following trend is observed from their phase diagram (Figure 8). In all mesophases, the two enantiomeric structural units of the monomers are miscible and isomorphic over the entire range of compositions. Regardless of the history of the DSC scan from which the experimental data are collected,

Table 7. Characterization of the Binary Mixtures of Poly[(*R*)-8] (DP = 16.3, M_w/M_n = 1.14) with Poly[(*S*)-8] (DP = 15.2, M_w/M_n = 1.15) (Polymer Mixture IV)[a]

poly[(*R*)-8]/poly[(*S*)-8] (mol/mol)	phase transitions (°C) and corresponding enthalpy changes (kcal/mru)	
	heating	cooling
0/100	K 80.4 (1.14) S_X 90.8 (0.22) S_C* 112.9 (1.45) I	I 108.1 (−1.51) S_C* 87.8 (−0.14) S_X 70.0 (−0.71) K
14.0/86.0	K 79.3 (1.11) S_X 90.2 (0.25) S_C* 112.9 (1.38) I	I 108.2 (−1.46) S_C* 87.8 (−0.14) S_X 69.6 (−0.75) K
22.2/77.8	K 79.0 (1.12) S_X 89.9 (0.24) S_C* 113.2 (1.46) I	I 108.4 (−1.49) S_C* 87.8 (−0.14) S_X 69.7 (−0.73) K
39.5/60.5	K 78.6 (1.13) S_X 90.4 (0.26) S_C* 113.5 (1.45) I	I 108.6 (−1.51) S_C* 87.9 (−0.13) S_X 69.7 (−0.74) K
49.9/50.1	K 78.5 (1.05) S_X 90.0 (0.26) S_C* 113.5 (1.45) I	I 108.7 (−1.44) S_C* 87.8 (−0.13) S_X 69.6 (−0.74) K
59.7/40.3	K 78.7 (1.07) S_X 90.6 (0.21) S_C* 113.7 (1.46) I	I 108.9 (−1.43) S_C* 87.8 (−0.11) S_X 69.8 (−0.71) K
80.4/19.6	K 79.7 (1.08) S_X 91.7 (0.26) S_C* 114.1 (1.46) I	I 109.0 (−1.43) S_C* 88.5 (−0.11) S_X 70.1 (−0.73) K
89.5/10.5	K 80.2 (1.09) S_X 91.6 (0.27) S_C* 113.9 (1.46) I	I 109.1 (−1.38) S_C* 89.0 (−0.11) S_X 70.4 (−0.72) K
100/0	K 81.1 (1.09) S_X 92.7 (0.22) S_C* 114.1 (1.45) I	I 109.3 (−1.49) S_C* 89.6 (−0.17) S_X 71.1 (−0.74) K

[a] Data are from second heating and first cooling scans (10 °C/min).

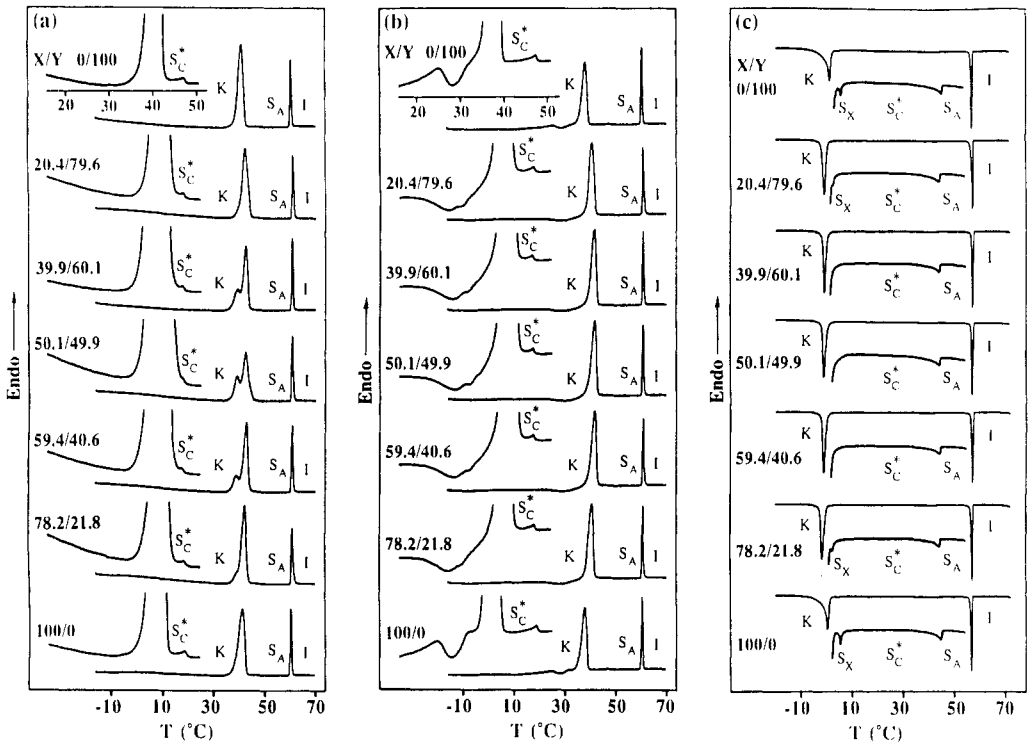

Figure 7. DSC thermograms (10 °C/min) of the binary mixtures of monomer (*R*)-8 (X) with monomer (*S*)-8 (Y): (a) first heating scans; (b) second heating scans; (c) first cooling scans.

the S_A–I transition temperature shows an upward curvature, i.e., a positive deviation (0.4 deg) from the linear dependence predicted by the Schröder–van Laar equation for an ideal solution,[19,20] demonstrating the presence of an interaction and, therefore, of chiral molecular recognition between the two enantiomeric structural units in the S_A phase. In contrast to the S_A–I transitions, the S_C*–S_A transition temperature shows a downward curvature, i.e., a negative deviation (−0.8 to −1.0 deg) from the ideal value. This result indicates a nonideal solution behavior and, therefore, the absence of any interaction between the two enantiomers, as well as the absence of chiral molecular recognition in the S_C* phase. The monotropic S_X phase is observed only in the high optical purity regions of the phase diagram (Figure 8c). It seems that the suppression of the S_X phase by mixing is so large that it turns into a virtual phase in the low optical purity region of the phase diagram. This is due to the immiscibility of the two enantiomers in this phase. In the heating scans, the melting transition shows an upward curvature with positive deviations from the ideal values (Figure 8a,b). The positive deviation of the melting temperature in the 50/50 mixture is 3.8 °C in the second (Figure 8b) and subsequent heating scans, and this indicates that the crystal structures of the two enantiomers are isomorphic, and in addition, a chiral recognition effect larger than that in the S_A phase is available in this crystalline phase. In systems in which the two crystal phases are not isomorphic and chiral recognition is not detected, a large suppression of the melting temperature with a eutectic point is observed. This was the case for the pairs of diastereomers and enantiomers reported in previous publications.[14,15] However, in the present system, the suppression of the crystallization temperature is partially canceled by the chiral recognition effect, resulting in a relatively small (−2.0 deg) negative deviation of the kinetically controlled crystallization temperature (Figure 8c).

In the four sets of polymer mixtures with different molecular weights, the two enantiomeric structural units derived from the two monomers are also miscible and isomorphic in all mesophases across the full composition range. The major difference between the monomer mixtures and the polymer mixtures is that the polymer system does not show a S_A phase, as discussed in detail in the previous section. Figure 9 presents a few selected examples of phase diagrams of polymer mixtures obtained from data collected during the second heating scan. The S_C*–I transitions of the polymer mixtures always show an upward curvature in all DSC scans for all molecular weights, and this behavior resembles that observed for

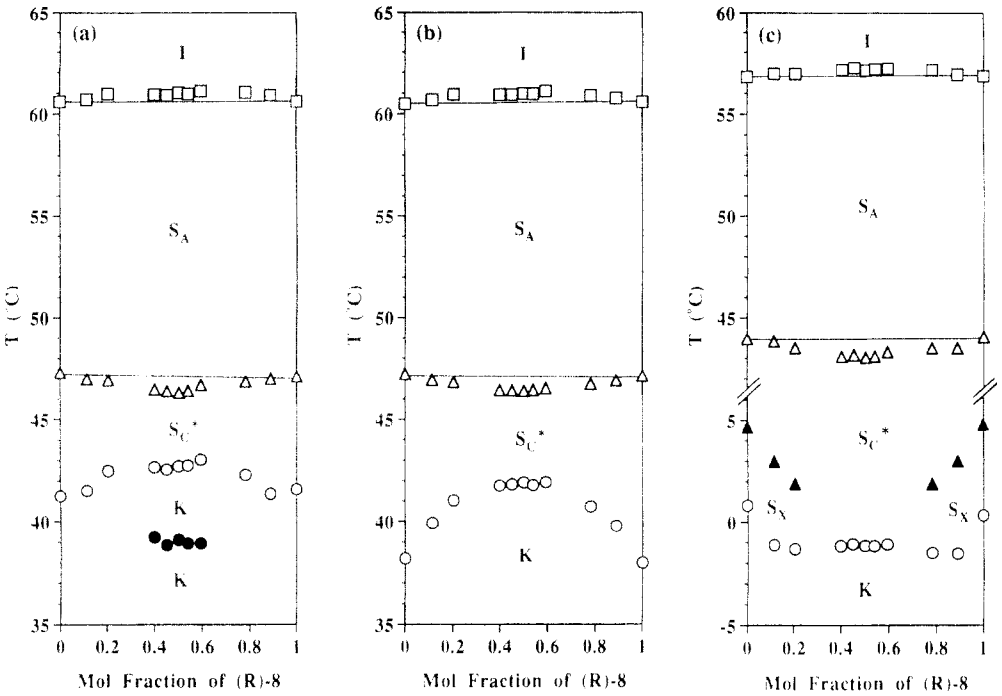

Figure 8. Dependence of phase transition temperatures on the composition of the binary mixtures of (*R*)-8 with (*S*)-8: (a) data from the first heating scans; (b) data from the second heating scans; (c) data from the first cooling scans.

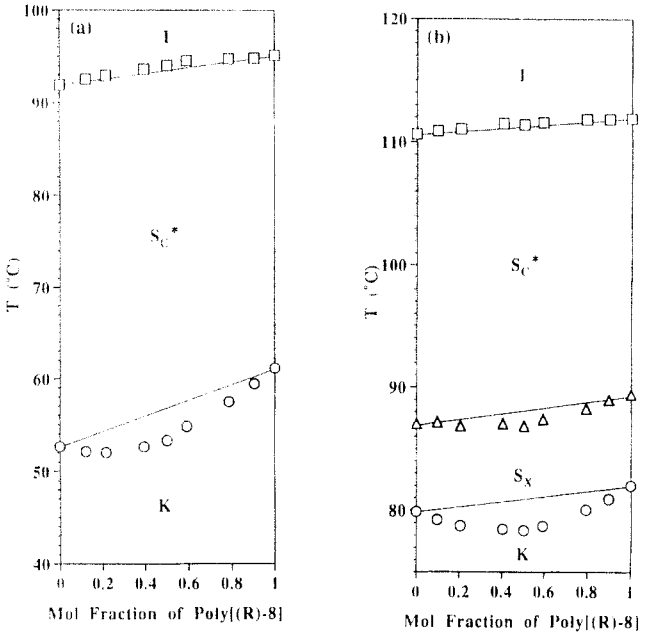

Figure 9. Dependence of transition temperatures obtained from the second heating scan on the composition of (a) polymer mixture I [poly[(*R*)-8] (DP = 5.6) and poly[(*S*)-8] (DP = 5.1)] and (b) polymer mixture III [poly[(*R*)-8] (DP = 13.2) and poly[(*S*)-8] (DP = 13.1)].

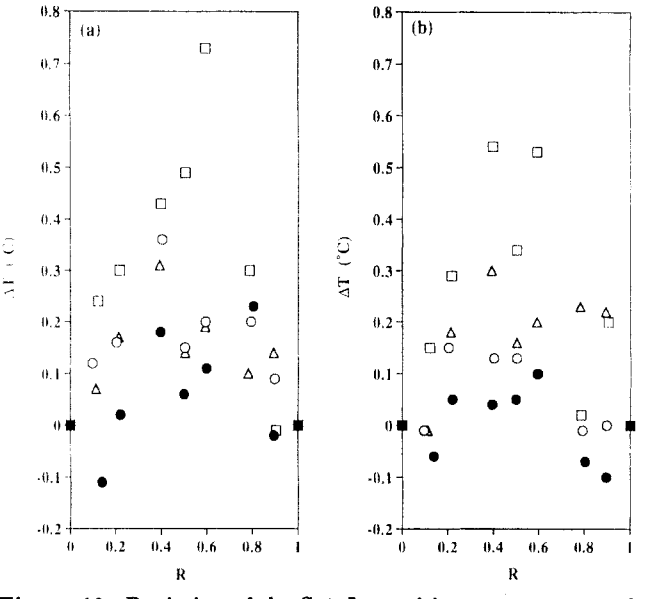

Figure 10. Deviation of the S_C^*–I transition temperatures of the polymer mixtures from the theoretical ideal values (ΔT) *versus* mixture composition: (a) data from the second heating scans; (b) data from the first cooling scans. Key: (●) polymer mixture IV; (○) polymer mixture III; (△) polymer mixture II; (□) polymer mixture I.

the S_A–I transitions in the monomer mixtures (Figure 8). A downward curvature was observed for the S_X–S_C^*, K–S_X, and K–S_C^* temperatures of all polymer mixtures. This behavior is similar to that observed for the S_C^*–S_A and S_X–S_C^* transitions of the monomer mixtures (Figure 8).

In order to compare the S_C^*–I transition temperatures quantitatively, the deviation from the theoretical value (ΔT) was calculated using the Schroeder–van Laar equation[19,20] for all the S_C^*–I transition temperatures obtained for the four sets of polymer mixtures. Figure 10 summarizes ΔT versus the composition of the mixture for the second heating and first cooling scans. Although the data points are fluctuating, a molecular weight dependence of the ΔT value is clearly observed from Figure 10: i.e., with increasing molecular weight from polymer mixtures I to IV, the ΔT values are decreasing. The largest ΔT value observed for polymer mixture I is *ca.* 0.5 deg, which is almost canceled to 0 deg in polymer mixture IV. These results demonstrate that chiral molecular interactions are present between the two enantiomeric structural units in the S_C^* phase and that the polymer backbone "effect" decreases this effect. The decrease of this effect is parallel with the increase of the polymer molecular weight.

Copolymerization of (*R*)-8 and (*S*)-8. Copolymerization of (*R*)-8 with (*S*)-8 was performed to cover the entire range of compositions. Attempts were made to synthesize poly[[(*R*)-8]-*co*-[(*S*)-8]] with DP = 20. Since the transition temperatures of polymers are strongly dependent on their molecular weight, it is essential to synthesize polymers

Table 8. Cationic Copolymerization of (*R*)-8 with (*S*)-8 and Characterization of the Resulting Polymers[a]

[(*R*)-8]/[(*S*)-8] (mol/mol)	polymer yield (%)	$10^{-3}M_n$	M_w/M_n	DP	phase transitions (°C) and corresponding enthalpy changes (kcal/mru) heating	cooling
0/100	75.7	6.01	1.13	12.8	K 73.9 (1.16) S_X 80.8 (0.16) S_C^* 107.0 (1.41) I	I 102.0 (−1.55) S_C^* 76.8 (−0.09) S_X 63.8 (−0.77) K
20/80	70.5	5.87	1.15	12.5	K 73.5 (1.16) S_X 81.1 (0.21) S_C^* 107.6 (1.49) I	I 102.6 (−1.55) S_C^* 78.3 (−0.12) S_X 63.9 (−0.77) K
40/60	71.2	6.06	1.16	12.9	K 72.7 (1.10) S_X 82.0 (0.24) S_C^* 108.3 (1.48) I	I 103.1 (−1.52) S_C^* 79.0 (−0.12) S_X 63.7 (−0.72) K
50/50	71.1	6.03	1.15	12.8	K 71.7 (1.07) S_X 81.4 (0.25) S_C^* 108.1 (1.48) I	I 103.2 (−1.53) S_C^* 78.4 (−0.12) S_X 63.4 (−0.72) K
60/40	69.6	6.06	1.14	12.9	K 71.8 (1.08) S_X 81.6 (0.27) S_C^* 108.1 (1.46) I	I 103.2 (−1.51) S_C^* 79.1 (−0.13) S_X 63.5 (−0.69) K
100/0	70.3	5.99	1.14	12.7	K 74.3 (1.18) S_X 81.4 (0.16) S_C^* 107.4 (1.44) I	I 102.1 (−1.50) S_C^* 78.1 (−0.11) S_X 64.0 (−0.76) K

[a] Conditions: polymerization temperature, 0 °C; polymerization solvent; methylene chloride; $[M]_0 = [(R)\text{-}8] + [(S)\text{-}8] = 0.224$; $[M]_0/[I]_0 = 20$; $[Me_2S]_0/[I]_0 = 10$; polymerization time, 1 h. Transition data are from second heating and first cooling scans (10 °C/min).

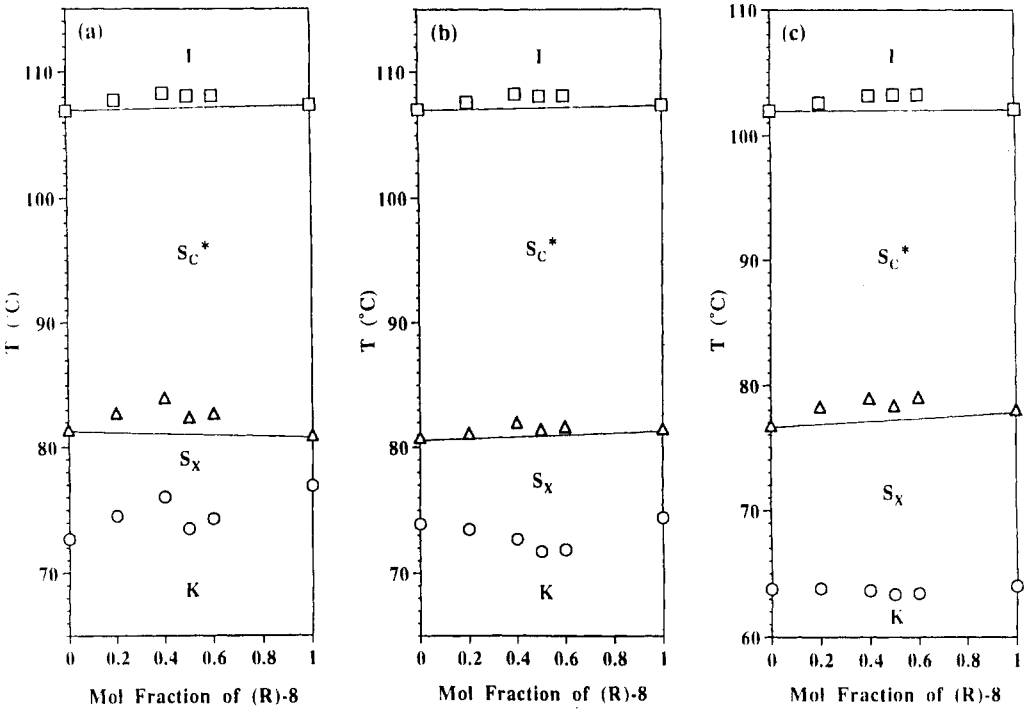

Figure 11. Dependence of the phase transition temperatures on the composition of poly[(*R*)-8-*co*-(*S*)-8] (DP = 12.5–12.9): (a) data from the first heating scans; (b) data from the second heating scans; (c) data from the first cooling scans.

having identical molecular weights in order to compare their transition temperatures. This can be achieved only by employing the living polymerization technique. The copolymerization results are listed in Table 8. The yields reported in Table 8 are lower than quantitative due to the polymer losses during the purification process. However, all conversions were quantitative and, therefore, since the two monomers provide an azeotropic copolymerization, the copolymer composition is identical to that of the monomer feed.[6] The average degree of polymerization determined by GPC is about 12.8.

The thermal transition temperatures determined by DSC are listed in Table 8 and the data from the first and second heating scan and first cooling scans are plotted against copolymer composition in Figure 11. The data points of poly[[(*R*)-8]-*co*-[(*S*)-8]] (0.8/0.2) are omitted since a slightly larger DP (13.8) was obtained only for this copolymer. These copolymers exhibit the same phase behavior as the mixture of their parent homopolymers over the entire range of compositions. The S_C^*–I transitions of the copolymers are higher than those of the homopolymers. The deviation in the 50/50 copolymer is *ca.* 1.0 deg, and this value is 5–10 times larger than that observed for the corresponding polymer mixtures with similar molecular weights (i.e., ΔT = 0.1–0.2 deg for polymer mixture III with DP = 13; see Figure 9b). Furthermore, the S_X–S_C^* transitions of the copolymers also show transition temperatures higher than those of the homopolymers. This copolymer behavior is in contrast to the behavior shown by the polymer mixtures in which the S_X–S_C^* transition is always suppressed by the mixing of the two enantiomeric polymers. These two observations demonstrate that there is a larger chiral molecular recognition between the two enantiomeric structural units in the copolymer system than in the corresponding polymer mixture. This copolymer is the first one from a large series of systems which provides such an effect. The results on other copolymer systems will be published elsewhere.

Summaries and Conclusions

The experimental results obtained from the miscibility studies on enantiomeric monomers reported in this paper are consistent with those obtained for the two previously reported systems.[14,15] In all these three systems including the current one, the 50/50 monomer mixture showed transition temperatures 0.4 deg higher and 0.5–1.0 deg lower than the corresponding ideal values for the S_A–I and S_C^*–S_A transitions, respectively. The transition involving higher order mesophases (S_X phase) shows larger negative deviations from the ideal value in the current system and in the diastereomeric system which was reported in the first publication.[14] These results show that chiral recognition always seems to exist in the untilted S_A phase if the two enantiomers are miscible, but not in the tilted S_C^* phase and in other higher order phases. The major difference of the current system from the previous two systems lies in the crystalline phase in which we observed a much larger chiral recognition effect than in the S_A phase. No definitive structure for this crystalline phase is available at the present time.

With regard to the polymer mixtures, it is difficult to compare the data from the three systems quantitatively because the nature of the transition is different (i.e., S_A–I versus S_C*–I). However, it is important to note that the current results provide the first example of heterochiral molecular recognition in the tilted S_C* phase. The chiral molecular recognition effect shows a very clear molecular weight dependence, which is completely different from the one observed in the similar enantiomeric system containing a chlorine atom in the chiral center.[15]

In the copolymerization studies, the precise control of molecular weight and polydispersity is most crucial for the quantitative comparison of transition temperatures. In this respect, the current investigations have achieved better control over the polymerization reaction than in previously investigated systems and very clear trends were observed for the S_C*–I and S_X–S_C* transitions. The positive deviation from the ideal values displayed by both transitions of the copolymer are larger than those observed in mixtures of monomers and polymers, and the explanation for this behavior may be related to the microstructure of the copolymer which favors the enantiomeric interaction.

Finally, the results obtained from these series of investigations show that each individual system studied gives unique mesomorphic behavior, and as a consequence, it is not yet possible to discuss quantitatively the influence of various structural parameters on the enantiomeric interactions. The only clear trend is that for the same stereocenter, enantiomeric interactions are strongly dependent on the nature of the liquid crystalline phase and for the same phase they are determined by the molecular and macromolecular structure of the enantiomer. Even if more extensive studies are required for this purpose, the results reported here have demonstrated that layered two-dimensional liquid crystalline phases provide an interesting alternative approach to quantitative studies on chiral molecular recognition which so far was performed only on two-dimensional monolayers of enantiomers[21] and diastereomers.[22]

Acknowledgment. Financial support by the Office of Naval Research and Asahi Chemical Industry Co., Ltd., Japan, is gratefully acknowledged. We also thank Professor S. Z. D. Cheng of the University of Akron for the X-ray measurements.

References and Notes

(1) (a) Lehn, J. M. *Struct. Bonding* **1973**, *16*, 1. (b) Lehn, J. M. *Angew. Chem., Int. Ed. Engl.* **1988**, *27*, 89. (c) Lehn, J. M. *Angew. Chem., Int. Ed. Engl.* **1990**, *29*, 1304. (d) Diederich, F. *Cyclophasnes*; Royal Society of Chemistry: Cambridge, U.K., 1991. (e) Buckingham, A. D.; Legon, A. C.; Roberts, S. M. *Principles of Molecular Recognition*; Chapman and Hall: London, 1993; p 1.

(2) (a) Collet, A.; Brienne, M. J.; Jaques, J. *Chem. Rev.* **1980**, *80*, 215. (b) Jaques, J.; Collet, A.; Wilen, S. H. *Enantiomers, Racemates and Resolutions*; Krieger: Malabar, 1991.

(3) (a) Pirkle, W. H.; Pochapsky, T. C. *Chem. Rev.* **1989**, *89*, 347. (b) Arnett, E. M.; Harvery, N. G.; Rose, P. L. *Acc. Chem. Res.* **1989**, *22*, 131. (c) Rose, P. L.; Harvey, N. G.; Arnett, E. M. In *Advances in Physical Organic Chemistry*; Bethel, D., Ed.; Academic Press: London, U.K., 1993; Vol. 28, p 45.

(4) (a) Goodby, J. W. *Science* **1986**, *231*, 350. (b) Goodby, J. W.; Blinc, R.; Clark, N. A.; Lagerwall, S. T.; Osipov, M. A.; Pikin, S. A.; Sakurai, T.; Yoshino, K.; Zeks, B. *Ferroelectric Liquid Crystals: Principles, Properties and Applications*; Gordon and Breach Science Publishers: Philadelphia, PA, 1991. (c) Goodby, J. W.; Nishiyama, I.; Slaney, A. J.; Booth, C. J.; Toyne, K. J. *Liq. Cryst.* **1993**, *14*, 37. (d) Escher, C.; Wingeen, R. *Adv. Mater.* **1992**, *4*, 189.

(5) (a) Bahr, C. H.; Heppke, G.; Sabaschus, B. *Liq. Cryst.* **1991**, *9*, 31. (b) Slaney, A. J.; Goodby, J. W. *Liq. Cryst.* **1991**, *9*, 849. (c) Takezoe, H.; Lee, J.; Chandani, A. D. L.; Gorecka, E.; Ouchi, Y.; Fukuda, A.; Terashima, K.; Furukawa, K. *Ferroelectrics* **1991**, *114*, 187. (d) Nguyen, H. T.; Twieg, R. J.; Nabor, M. F.; Isaert, N.; Destrade, C. *Ferroelectrics* **1991**, *121*, 187. (e) Leclercq, M.; Billard, J.; Jacques, M. *Mol. Cryst. Liq. Cryst.* **1969**, *8*, 367. (f) Bahr, C. H.; Heppke, G.; Sabaschus, B. *Ferroelectrics* **1988**, *84*, 103. (g) Yamada, Y.; Mori, K.; Yamamoto, N.; Hayashi, H.; Nakamura, K.; Yamawaki, M.; Orihara, H.; Ishibashi, Y. *Jpn. J. Appl. Phys.* **1989**, *28*, L1606. (h) Heppke, G.; Lötzsch, D.; Demus, D.; Diele, S.; Jahn, K.; Zaschke, H. *Mol. Cryst. Liq. Cryst.* **1991**, *208*, 9. (i) Takezoe, H.; Fukuda, A.; Ikeda, A.; Takanishi, Y.; Umemoto, T.; Watanabe, J.; Iwane, H.; Hara, M.; Itoh, K. *Ferroelectrics* **1991**, *122*, 167.

(6) For a brief review on the molecular engineering of side chain LCP by living cationic polymerization see: Percec, V.; Tomazos, D. *Adv. Mater.* **1992**, *4*, 548.

(7) (a) Percec, V.; Zheng, Q.; Lee, M. *J. Mater. Chem.* **1991**, *1*, 611. (b) Percec, V.; Zheng, Q.; Lee, M. *J. Mater. Chem.* **1991**, *1*, 1015. (c) Percec, V.; Zheng, Q. *J. Mater. Chem.* **1992**, *2*, 475. (d) Percec, V.; Zheng, Q. *J. Mater. Chem.* **1992**, *2*, 1041.

(8) (a) Olah, G. A.; Welch, J. *Synthesis* **1974**, 652. (b) Olah, G. A.; Welch, J. T.; Vankar, Y. D.; Nojima, M.; Kerekes, I.; Olah, J. A. *J. Org. Chem.* **1979**, *44*, 3872. (c) Keck, R.; Rétey, J. *Helv. Chim. Acta* **1980**, *63*, 769. (d) Olah, G. A.; Prakash, G. K.; Chao, Y. L. *Helv. Chim. Acta* **1981**, *64*, 2528. (e) Faustint, F.; Munari, S. D.; Panzeri, A.; Villa, V.; Gandolfi, C. A. *Tetrahedron Lett.* **1981**, *22*, 4533. (f) Barber, J.; Keck, R.; Rétey, J. *Tetrahedron Lett.* **1982**, *23*, 1549.

(9) Fu, S. J.; Birnbaum, S. M.; Greenstein, J. P. *J. Am. Chem. Soc.* **1954**, *76*, 6054.

(10) (a) Sierra, T.; Meléndez, E.; Serrano, J. L.; Ezcurra, A.; Pérez-Jubindo, M. A. *Chem. Mater.* **1991**, *3*, 157. (b) Sierra, T.; Serrano, J. L.; Ros, M. B.; Ezcurra, A.; Zubía, J. *J. Am. Chem. Soc.* **1992**, *114*, 7645. (c) Sierra, T.; Ros, M. B.; Omenat, A.; Serrano, J. L. *Chem. Mater.* **1993**, *5*, 938.

(11) (a) Yoshino, K.; Kishio, S.; Ozaki, M.; Sakurai, T.; Mikami, N.; Higuchi, R.; Honma, M. *Jpn. J. Appl. Phys.* **1986**, *25*, L416. (b) Yoshino, K.; Ozaki, M.; Kishio, S.; Sakurai, T.; Mikami, N.; Higuchi, R.; Honma, M. *Mol. Cryst. Liq. Cryst.* **1987**, *144*, 87. (c) Ozaki, M.; Yoshino, K.; Sakurai, T.; Mikami, N.; Higuchi, R. *J. Chem. Phys.* **1987**, *86*, 3648.

(12) (a) Twieg, R. J.; Betterton, K.; Nguyen, H. T.; Tang, W.; Hinsberg, W. *Ferroelectrics* **1989**, *91*, 243. (b) Shivkumar, B.; Sadashiva, B. K.; Krishna Prasad, S.; Khened, S. M. *Ferroelectrics* **1991**, *114*, 273.

(13) See for example: Tsuji, H.; Ikada, Y. *Macromolecules* **1993**, *26*, 6918 and references cited therein.

(14) Percec, V.; Oda, H.; Rinaldi, P. L.; Hensley, D. R. *Macromolecules* **1994**, *27*, 12.

(15) Percec, V.; Oda, H. *Macromolecules*, in press.

(16) Booth, C. J.; Goodby, J. W.; Hardy, J. P.; Lettington, O. C.; Toyne, K. J. *J. Mater. Chem.* **1993**, *3*, 821.

(17) (a) Percec, V.; Lee, M.; Jonsson, H. *J. Polym. Sci., Part A: Polym. Chem.* **1991**, *29*, 327. (b) Percec, V.; Lee, M. *Macromolecules* **1991**, *24*, 1017. (c) Percec, V.; Lee, M.; Rinaldi, P.; Litman, V. E. *J. Polym. Sci., Part A: Polym. Chem.* **1992**, *30*, 1213.

(18) (a) Cho, C. G.; Feit, B. A.; Webster, O. W. *Macromolecules* **1990**, *23*, 1918. (b) Cho, C. G.; Feit, B. A.; Webster, O. W. *Macromolecules* **1992**, *25*, 2081. (c) Lin, C. H.; Matyjaszewski, K. *Polym. Prepr. (Am Chem. Soc., Div. Polym. Chem.)* **1990**, *31*, 599.

(19) (a) Van Hecke, G. R. *J. Phys. Chem.* **1979**, *83*, 2344. (b) Achard, M. F.; Mauzac, M.; Richard, H.; Sigaud, G.; Hardouin, F. *Eur. Polym. J.* **1989**, *25*, 593.

(20) (a) Percec, V.; Lee, M. *J. Mater. Chem.* **1991**, *1*, 1007. (b) Percec, V.; Lee, M.; Zheng, Q. *Liq. Cryst.* **1992**, *12*, 715. (c) Percec, V.; Johansson, G. *J. Mater. Chem.* **1993**, *3*, 83.

(21) (a) Arnett, E. M.; Harvey, N. G.; Rose, P. L. *Acc. Chem. Res.* **1989**, *22*, 131. (b) Rose, P. L.; Harvey, N. G.; Arnett, E. M. In *Advances in Physical Organic Chemistry*, Bethell, D., Ed.; Academic Press: New York, 1993; Vol. 28, p 45. (c) Arnett, E. M.; Thompson, O. *J. Am. Chem. Soc.* **1981**, *103*, 968. (d) Harvey, N. G.; Rose, P. L.; Mirajovsky, D.; Arnett, E. M. *J. Am. Chem. Soc.* **1990**, *112*, 3547. (e) Arnett, E. M.; Gold, J. M. *J. Am. Chem. Soc.* **1982**, *104*, 636. (f) Qian, P.; Matsuda, M.; Miyashita, T. *J. Am. Chem. Soc.* **1993**, *115*, 5624.

(22) (a) Harvey, N.; Rose, P.; Porter, N. A.; Huff, J.; Arnett, E. M. *J. Am. Chem. Soc.* **1988**, *110*, 4395. (b) Heath, J. G.; Arnett, E. M. *J. Am. Chem. Soc.* **1992**, *114*, 4500.